Miniaturization Limits for Single-Chamber Micro Solid Oxide Fuel Cells with Coplanar Electrodes

Melanie Kuhn [a,*], Teko W. Napporn [b,1], Michel Meunier [b], Srikar Vengallatore [c], and Daniel Therriault [a]

[a]*Department of Mechanical Engineering, École Polytechnique de Montréal, Montreal, Quebec, H3C 3A7, Canada*

[b]*Department of Engineering Physics, École Polytechnique de Montréal, Montreal, Quebec, H3C 3A7, Canada*

[c]*Department of Mechanical Engineering, McGill University, Montreal, Quebec, H3A 2K6, Canada*

* Corresponding author. Tel.: +1 514 340 4711 ext. 7408; fax: +1 514 340 4176.

E-mail address: melanie.kuhn@polymtl.ca (M. Kuhn).

[1] Present address: Equipe Electrocatalyse, LaCCO, UMR CNRS 6503, Université de Poitiers, 86022 Poitiers Cedex, France

Abstract:

Single-chamber solid oxide fuel cells with coplanar microelectrodes were operated in methane-air mixtures (R_{mix} = 2) at 700°C. The performance of cells with one pair of NiO-YSZ (yttria stabilized zirconia) anode and $(La_{0.8}Sr_{0.2})_{0.98}MnO_3$-YSZ cathode, arranged parallel on a YSZ electrolyte substrate, was found to be significantly dependent on the electrode width. For an interelectrode gap of ~250 μm, cells with average electrode widths exceeding ~850 μm could establish a stable open circuit voltage (OCV) of ~0.8 V, while those with widths less than ~550 μm could not establish any OCV. In the intermediate range, the cells exhibited significant fluctuations in voltage and power under our testing conditions. This behavior suggests that a lower limit to electrode dimensions exists for cells with single electrode pairs, below which neither a stable difference in oxygen partial pressure, nor an OCV, can be established. Conversely, increasing the electrode width imposes a penalty in the form of an increase in the ohmic resistance. However, both size limits can be circumvented by employing multiple pairs of microscale electrodes in an interdigitated configuration.

Keywords: Solid oxide fuel cell; Single chamber; Micro cell; Coplanar electrodes; Ceramic materials

1. Introduction

Single-chamber solid oxide fuel cells (SC-SOFCs) are operated in uniform mixtures of fuel and oxidant gases, whereas conventional dual-chamber SOFCs rely on the strict separation of the two reactant gases [1, 2]. In SC-SOFCs, the selectivity of the electrodes for catalyzing the reaction of the respective gas, that is, the anode for the fuel oxidation and the cathode for the oxidant reduction, enables the generation of an electrical power output. The use of a single gas chamber and reactant gas mixtures eliminates the challenges of separate gas manifolding and high-temperature gas-tight sealing, which enables simple and compact designs for SC-SOFCs and makes these devices attractive for miniaturized portable power generation. Additionally, single-chamber operation permits the development of new cell designs such as fully-porous cells [3] and single-face cells with coplanar electrodes located on the same side of the electrolyte [4-11], neither of which is possible under dual-chamber conditions.

The single-face configuration was first mentioned by van Gool in 1965 [12] in connection with the possibility of surface ionic migration between adjacent coplanar electrodes in fuel cells. This idea was later adapted in a patent by Louis et al. in 1981 [13], but it was not until the early 1990s that the feasibility of SOFCs with coplanar electrodes operating in fuel-air mixtures was experimentally demonstrated by Hibino et al. [4, 5]. In conventional three-layer electrode-electrolyte-electrode designs, the thickness of the electrolyte determines the ohmic resistance to the conduction of oxygen ions from cathode to anode through the electrolyte, so that reducing the electrolyte thickness leads to a reduction of the ohmic losses. In the single-face design, the oxygen ions travel from one electrode to the other through the gap, bridged by the electrolyte, between the electrodes

[5]. The ohmic resistance can thus be reduced by decreasing the interelectrode distance without the need for ultrathin electrolytes. Thick, mechanically strong electrolyte substrates can be employed, onto which multiple single cells can be fabricated and be connected in series or parallel [5, 7, 8]. The conduction path and the ohmic resistance can further be decreased by reducing the electrode width [5, 7], as only a small part of the electrode closest to the gap and the opposite electrode appears to be active for the electrochemical reactions [7, 8].

Although it has repeatedly been shown that reducing interelectrode distance and electrode width leads to higher cell performance [4-7, 9], no study has yet determined the ultimate limits on gap and width at which SC-microSOFCs (SC-μSOFCs) with coplanar electrodes can still be operated. Most SC-μSOFC studies report on cells consisting of one pair of parallel electrode lines with interelectrode gap and electrode width ranging from a few hundred micrometers to a few millimeters. Over this range, the highest power was obtained for the smallest of these cells, with interelectrode gaps and electrode widths of 0.5 mm and 1 mm [4-6], 0.255 mm and ~0.6 mm [9], and 0.2 mm and 0.5 mm [7], respectively. There is a general consensus that further reduction to microscale sizes could further improve performance. Results from modeling predicted optimal performance for interelectrode gaps of 10 μm and electrode widths of 20 μm [14], or 6 to 10 μm wide electrodes spaced 2 μm apart [15]. However, micrometer-sized gaps might induce intermixing of reactant gases and reaction products, which could limit the electrochemical performance of the cell [9, 16]. The low open circuit voltage (OCV) of 380 mV and the poor stability of a SC-μSOFC with an interelectrode gap of 5 μm and electrode widths of

15 μm [17] indicates that reduced electrode feature sizes can degrade cell performance. To some extent, this degradation can be mitigated by employing multiple lines per electrode in an interdigitated configuration [8, 10, 11, 18]; for instance, cells containing interdigitated electrodes with electrode widths of 100 μm and spacings of 10 μm exhibited OCVs of 0.65 V and power densities of a few mW cm^{-2} [8].

The aim of this study is to investigate the existence of a limit to the miniaturization of SC-μSOFCs with one pair of coplanar electrodes, and whether such a limit can be overcome by increasing the number of electrode lines in the form of interdigitated electrode patterns or by using cell stacks. Conventional SOFC materials, i.e., nickel oxide - yttria stabilized zirconia (NiO-YSZ) for the anode, lanthanum strontium manganate (LSM)-YSZ for the cathode and YSZ for the electrolyte, were used to fabricate and test cells with one line per anode and cathode with average electrode widths ranging from 93 to 1380 μm, and with an interelectrode gap of ~250 μm. Subsequently, cells with one, two, three, four, five and ten electrode pairs in an interdigitated pattern with line widths of ~260 μm were tested to evaluate the effect of the number of electrode lines on cell performance. Finally, the performance of stacks composed of two to three cells, with either one pair or five electrode pairs per cell, was measured to assess the impact of stacking on cell performance.

2. Experimental

2.1 SC-μSOFC fabrication

The coplanar electrodes were fabricated using a robot-controlled direct-write microfabrication technique consisting of the pressure-driven extrusion of electrode inks

through micronozzles and their deposition onto the electrolyte substrate [9-11, 19, 20]. NiO-YSZ and LSM-YSZ were used for the anode and cathode, respectively. The characteristics of the electrode materials are listed in Table I. The particle size and the specific surface area were provided by the supplier (NexTech Materials, Ltd., Lewis Center, OH), and the powder density was obtained using a He-Pycnometer AccuPyc 1330 (Micromeritics Instrument Corporation, Norcross, GA). The NiO-YSZ mixture was prepared by mixing NiO and YSZ in a weight ratio of 55 wt% to 45 wt%, followed by ball milling for 8 hours in a Spex CertiPrep 8000M Mixer/Mill (Spex CertiPrep, Metuchen, NJ). For the ink fabrication, Triton (Alfa Aesar, Ward Hill, MA) was added to the respective electrode powder as a dispersant, and the two ingredients were ball milled for 10 min in the Spex Mixer/Mill with YSZ balls (0.5 and 1.0 mm in diameter) as milling media. A mixture of fully dissolved binder (Poly(vinyl butyral-co-vinyl alcohol-co-vinyl acetate), Sigma-Aldrich, St. Louis, MO) and organic solvent (Terpineol, Mallinckrodt Baker, Inc., Phillipsburg, NJ) was then added for thorough mixing for 1 hour in the Spex Mixer/Mill. The solid loading of the different electrode inks ranged from 16 to 18 vol%.

The electrode inks were then extruded under air pressure (Ultra^{TM} 2400 Series, EFD, Inc., East Providence, RI) through stainless steel micronozzles (EFD, Inc., East Providence, RI). A robotic direct-write deposition apparatus (I&J 2200-4, I&J Fisnar, Inc., Fair Lawn, NJ) was used for their deposition onto the 0.2 mm thick YSZ (8 mol% Y_2O_3) electrolyte (Marketech International, Inc., Port Townsend, WA). SC-μSOFCs with single electrode pairs as well as interdigitated electrode patterns with two, three, four, five and ten lines per electrode were fabricated (see Fig. 1 a-d). Micronozzles of different diameters

(inner nozzle diameter: 0.1 - 0.61 mm) were used to deposit single electrode pairs of different electrode width. The electrodes were co-sintered under ambient atmosphere for 3 hours at 1200°C.

The electrode width and length, interelectrode distance, and electrode surface area were measured from optical micrographs captured using an Olympus SZX12 stereomicroscope (Olympus Cooperation, Tokyo, Japan) and analyzed by using digital imaging software (Image-Pro Plus 6.2, Media Cybernetics, Inc., Bethesda, MD). The electrode microstructure was characterized by scanning electron microscopy (ESEM, Quanta FEG 200, FEI Company, Hillsboro, OR). The electrode thickness was measured from SEM images of the cross-sectional view of the sliced electrodes and corresponds to the maximum thickness of the lens-like cross-sectional shape of the electrodes [11].

2.2 Electrochemical characterization

The SC-μSOFCs were characterized using a high-temperature testing setup [10, 11, 20-22]. A gas distribution plate was used based on the design described in Ref. [23], but modified to suit the needs of testing single-chamber fuel cells with coplanar electrodes. The cells were placed on a support plate inside the cell holder, and current collectors and gas distribution plate were installed over the coplanar electrodes (see Fig. 2a). The gas distribution plate with open design [23] contained holes to let the reaction gases pass through it and access the cell underneath (Fig. 2b). Posts were machined on the surface of the gas distribution plate facing the cells to enhance mixing of the gases flowing over the electrodes.

The cells were tested in the single-chamber mode at 700°C using a methane-air mixture with a methane-to-oxygen ratio, R_{mix} = 2. Synthetic air, composed of nitrogen and oxygen in a ratio of 4 to 1, was used. The total flow rate of the gas mixture was 150 sccm. Additional nitrogen (with a flow rate of about 700 sccm) was used in the quartz tube around the cell holder to flush away the gases leaving the cell holder, and to prevent any counter gas diffusion. Before starting the electrochemical test and supplying oxygen into the system, the NiO anode was reduced in a methane-nitrogen mixture. The cells were positioned perpendicular to the direction of the gas flow, with the cathode being the first electrode to be exposed to the incoming gas mixture. This configuration has been identified to yield the highest power and OCV for SC-SOFCs with one single pair of coplanar electrodes [7]. Although SC-SOFC stacks have been reported to yield the highest power output for parallel gas flow [7], the perpendicular flow direction with cathode first was used throughout this study to permit direct comparison between single electrode pairs, interdigitated electrodes, and cell stacks. Gold wire (0.25 mm diameter, 99.9% metals basis, Alfa Aesar, Ward Hill, MA) and mesh (82 mesh, woven from 0.06 mm diameter wire, 99.9% metals basis, Alfa Aesar, Ward Hill, MA) were used for current collection. The gold grid was fixed with gold paste (C5450, Heraeus Holding GmbH, Hanau, Germany) over the electrode extremities in the case of the single electrode lines, and on the segment connecting the interdigitated electrodes. We have previously established that current collection on the whole electrode surface reduced activation and ohmic polarization, and led to higher performance, compared with current collectors placed only over the connecting pads [20]. However, the small size of the interdigitated electrodes makes it difficult to apply gold grids over the whole anode and cathode, respectively, without

causing internal short circuits. Therefore, and in order to eliminate effects due to variations in current collection method, the same current collection configuration was used for all cells. Fig. 1 e-f shows the typical cell and current collection configuration for stacks of three single cells.

The voltage was recorded using a data acquisition set (Agilent 34970A, Agilent Technologies, Santa Clara CA) in combination with the HP BenchLink Data Logger software (Agilent Technologies, Santa Clara CA). The voltage-current characteristics of the cell were obtained by varying the resistance on a decade resistor (Type 1432-M, General Radio Company, Cambridge, MA) and reading the voltage as well as the current (197 Autoranging Microvolt DMM, Keithley Instruments, Inc., Cleveland, OH) value. For all cells, the data for the plots of OCV against time were recorded immediately after the oxygen gas was turned on.

3. Results and Discussion

3.1 Effect of electrode width on cell performance

In order to investigate the effect of electrode size on the performance of SC-μSOFCs with coplanar electrodes, cells with one line per anode and cathode of different electrode width and similar interelectrode gap were fabricated. Table II summarizes the geometrical characteristics, OCV and power output of these cells. The electrode width and interelectrode distance were obtained as the average of 20 equidistant measurements (pixel size of 7 μm) over the whole length of the electrode and of the interelectrode gap, respectively. The mean values with standard deviation given in Table II for anode and

cathode widths, as well as the interelectrode gap, therefore also take into account the tapered electrode edges (see Fig. 1b), and the variations of electrode width and interelectrode gap of any specific cell are due to the electrode shape being not perfectly rectangular. The average interelectrode gap of all cells was ~250 μm, but the variations of the gap between the different cells are due to the limitations of the direct-writing technique using electrode inks with Newtonian flow behavior [9-11]. The reduced control of the electrode feature sizes also made it difficult to obtain cells with average electrode widths between 700 and 1000 μm, which is the reason for the uneven distribution of electrode widths reported in Table II. The electrode length was ~0.6 cm for all cells. Cells 1 to 8 exhibited an average electrode thickness between 4 to 14 μm, whereas the other cells were ~35 μm thick as a result of the use of nozzles with different diameters during direct-write deposition. For reasons discussed later, these variations in electrode thickness are not a significant factor in this study.

During the electrochemical testing of the different cells with a single electrode pair at 700°C, R_{mix} = 2 and a total gas flow rate of 150 sccm, three performance regimes with respect to the electrode width were identified and are represented by the stability of the OCV as a function of time in Fig. 3 for selected cells. A zero OCV was measured for a cell with very small electrodes with an average electrode width below 100 μm. A non-zero, but unstable and fluctuating OCV was obtained for a cell with ~550 μm wide electrodes, and only a cell with larger electrodes permitted the generation of a stable OCV of over 800 mV.

This dependence of the OCV on the average electrode width is summarized in Fig. 4a for all the tested cells with one pair of electrodes. Cells with average electrode widths

exceeding ~850 μm delivered stable OCVs above 0.8 V. A slight increase of the OCV from 0.8 V to 0.86 V was also observed as the electrode width decreased from 1380 μm to 847 μm. For cells with an average electrode width of ~550 μm, the OCV became unstable and exhibited significant fluctuations. Maximum, mean and minimum OCV are plotted in Fig. 4a for these cells to illustrate the voltage fluctuations, and the value in Table II corresponds to the maximum value measured during the OCV fluctuations. Finally, cells with electrode widths smaller than ~550 μm could not establish any significant OCV. Tests conducted at different gas flow rates (50 to 450 sccm), different R_{mix} values and different gas flow directions (parallel gas flow and perpendicular gas flow with anode first) led to the same result: a stable, non-zero OCV could not be established for these cells. A zero OCV was also measured for cells with a single pair of electrodes with average electrode widths between 300 and 400 μm, composed of different electrode material combinations (NiO-YSZ or NiO-$Ce_{0.9}Gd_{0.1}O_{1.95}$ for the anode, and LSM-YSZ, LSM or $(La_{0.6}Sr_{0.4})_{0.995}(Fe_{0.8}Co_{0.2})O_3$ for the cathode) and tested under the same conditions.

Similarly, the power output was also significantly influenced by the electrode width (Fig. 4b). Due to a zero OCV, cells with small electrode widths below 550 μm did not yield any power output. For cells with electrode widths of ~550 μm, power fluctuations were observed; the maximum, mean and minimum values of the cell power output are given in Fig. 4b, and the maximum value is reported in Table II. In the case of larger electrodes, a stable power could be measured. However, despite stable OCV and power, cells with the largest electrodes showed the lowest power among the cells with measurable power output. This behavior suggests that decreasing the electrode width leads to a decrease in the

conduction path and ohmic resistance [5-7], and a corresponding increase in the power. The increase in cell performance with decreasing electrode width is also shown in the voltage-current characteristics in Fig. 5a and b. For the unstable cells, the maximum values of measured voltage and current were used to plot the corresponding curves. Decreasing the average electrode width from 1380 to 847 μm led to an increase of power by more than three times. Further reduction of the electrode width led to an additional increase in power, but the instability and voltage and current fluctuations during testing made stable and repeatable operation impossible (Fig. 5a and b).

The aforementioned results suggest the existence of a critical electrode width, w_{critical}, around which voltage and current fluctuations are occurring, and below which stable cell operation is not possible. Three different regimes can thus be identified for cells with a single anode and cathode line: stable OCV (and cell power) for large electrodes ($w > w_{\text{critical}}$), fluctuating OCV (and cell power) for electrodes with a width near the critical value ($w \approx w_{\text{critical}}$) and zero OCV (and cell power) for small electrodes ($w < w_{\text{critical}}$).

Voltage fluctuations have been reported to occur in the case of SOFCs operated under single-chamber conditions [10, 20, 24, 25]. Oxidation-reduction cycles of the nickel catalyst in methane-air mixtures were identified as a source of fluctuations of temperature, gas composition, product concentration and voltage. However, it is unlikely that those cycles should be at the origin of the voltage fluctuations observed in this study. The measured voltage fluctuations not only occurred at a much shorter time scale (within seconds) as compared to the long-time (several hours to days) observations in the literature, but they should also be expected to occur for all cells with nickel-based anodes,

independently of the electrode size. In particular, the larger electrodes with an increased content of nickel should be expected to undergo nickel oxidation-reduction cycles. As the latter do not exhibit any voltage fluctuations over the short time scale, other sources for the fluctuations, including electrode size effects, must be considered.

The OCV is established due to a difference in oxygen partial pressure between anode and cathode, according to the Nernst equation:

$$\mathrm{OCV} = \frac{RT}{nF} \ln \frac{p_{O_{2,\mathrm{cathode}}}}{p_{O_{2,\mathrm{anode}}}} \tag{1}$$

where R is the gas constant, T the temperature, F the Faraday constant, n the number of electrons and p_{O2} the partial pressure of oxygen at each electrode. In the case of SC-SOFCs, this difference in oxygen partial pressure is generated by the different catalytic activity and selectivity of the anode and cathode for the respective electrode reactions [26]. However, electrode selectivity is a known problem in SC-SOFCs [27]. The anode and cathode have been shown to be not completely selective for their respective reactions, leading to lower voltage and power outputs as compared to conventional SOFCs [27], as well as low cell efficiencies [16].

The generation of the OCV depends on the oxygen partial pressure at the electrode-electrolyte interface, and thus the interfacial or active surface area and the number of available reaction sites. This area corresponds to the electrode area with a direct interface to the electrolyte. For electrodes of constant length, as in the case of the different tested cells of this study, the interfacial area is proportional to the electrode width. A large electrode width thus leads to a large interface, which is favorable for the generation of the OCV. Therefore, the electrode width must be considered as a primary variable to correlate with

the measured changes in the OCV. In contrast, the manufacturing-induced variations in electrode thickness (ranging from 4 to 40 μm) are not a significant factor, as the difference of oxygen partial pressure necessary for the generation of the OCV is established at the electrode-electrolyte interface, and therefore depends on the thickness of the interface and not on the electrode thickness. The thickness of this interface is expected to be the same for all cells because they were manufactured using the same materials and under identical processing conditions. Moreover, the interface thickness (or effective reaction zone) of a Ni-YSZ anode has been reported to be less than 1 micrometer [28], which is significantly less than the thickness of the electrodes in this study, and all the electrodes exhibit a porous microstructure. The generation of the OCV, which is an equilibrium state phenomenon, does not depend on gas transport through the thickness of the porous electrodes. The transport properties and thickness effects are expected to be important only when current is drawn from the cell because they play a role in electrode polarization losses [29].

Additionally, any effects due to intermixing of gases [9, 15] and impeded access of reactant gases to catalytic sites are considered to be comparable for all cells, because the interelectrode gaps are similar within the manufacturing tolerances. For these reasons, we believe that the observed changes in OCV correlate directly with electrode width for all the cells reported in this study.

Our results show that below a critical electrode width, stable cell operation is no longer possible for cells with single electrode pairs. This minimum size is expected to be a function of the testing conditions and cell materials used. In the case of Ni-YSZ anodes and LSM-YSZ cathodes on a YSZ electrolyte characterized under the testing conditions

described earlier, the critical width was identified to be ~550 μm for an average interelectrode gap of ~250 μm. Below the critical width, the electrodes are too small to establish a sufficient gradient of oxygen partial pressure and promote the electrode reactions. An electrode width close to the critical size would enable high power outputs, but the small electrode surface areas and the amount of catalyst are still insufficient to maintain a constant difference in oxygen partial pressure and continuously sustain the reactions. Stable conditions can thus only be obtained for larger electrodes with an increased interfacial or active electrode area.

In addition to the miniaturization limit, there is also an upper limit of useful electrode width, $w_{\text{effective}}$. As shown in Fig. 5a, the ohmic resistance, represented by the slope of the *E-I* curve, increases with increasing electrode width while the cell performance decreases. Previous studies have shown that the anodic area active for electrochemical reactions was located closest to the interelectrode gap, and the rest of the anode did not contribute significantly to the cell performance due to an increased ionic conduction path and ohmic resistance [7, 8]. One indication of this was that the active anode region appeared white in color after testing due to an enhanced loss of nickel catalyst. In this study, such a white region close to the interelectrode gap and at the anode tip was observed only for cells with average electrode widths of 847 μm and larger (Fig. 6a). As reported in Ref. [8], SEM characterization confirmed the partial loss of nickel in this region (Fig. 6c), whereas metallic nickel was found on the remaining anode surface (Fig. 6b). The other cells exhibited an anode microstructure similar to the one in Fig. 6b after testing.

Fig. 7 provides a graphical summary of the effects of electrode width on the performance of SC-μSOFCs with one coplanar pair of electrodes. In this graph, the maximum cell power output is plotted against the electrode width, *w,* and three performance regimes are identified. The first regime corresponds to a zero OCV and zero power output for cells with electrodes smaller than $w_{critical}$. The unstable regime is characterized by voltage and power fluctuations for cells with electrodes of width near $w_{critical}$. Stable power is obtained for cells with $w > w_{critical}$, but the increase in ohmic resistance with increasing electrode width ($w > w_{effective}$) continuously reduces the cell power output. Optimized performance can be obtained for electrode widths within the range $w_{critical} < w < w_{effective}$, which, under our testing conditions, was located between ~550 and 850 μm.

3.2 Effect of number of electrode lines

Numerous reports of successful operation of SC-SOFCs with multiple pairs of microelectrodes have been reported in the literature [8-11, 18]. Therefore, it is of interest to enquire whether such structures are also subjected to the size limits found for cells with a single pair of electrodes. Cells with one, two, three, four, five and ten pairs of electrodes with widths of ~260 μm, thickness of ~17 μm and interelectrode gaps of ~114 μm were fabricated and tested. As previously shown, the cell with one line per electrode did not yield any OCV (Fig. 8a). However, a non-zero OCV could be obtained as the number of electrode lines increased. A cell with two lines per electrode delivered a very low OCV of only ~0.2 V, which then decreased gradually to zero after about 10 minutes. A further

increase of the OCV was measured for a cell with three electrode pairs. The voltage showed periodic fluctuations between 0.4 and 0.6 V. Higher OCVs of ~0.8 V could then be obtained by further increasing the number of electrode lines (Fig. 8b). While cells with four lines per electrode still exhibited significant voltage drops and fluctuations, the amplitude of fluctuations decreased for cells with five and ten electrode pairs. These observations confirm that a higher and more stable OCV can be obtained for SC-μSOFCs with multiple pairs of coplanar interdigitated microelectrodes, thereby relaxing the size limits imposed on a single pair of microelectrodes and enabling the use of closely-spaced microelectrodes for reduced ohmic cell resistance.

The stability of the OCV was shown to improve with an increasing number of electrode lines and thus an increasing interfacial or active electrode area, while a constant electrode thickness of ~17 μm was maintained between the different cells. These results provide further evidence to support the previously mentioned conclusion that the OCV is a function of electrode width and active interfacial area, and not dependent on the thickness of the electrodes, in the fuel cells tested in this study. While one pair of electrodes smaller than the critical width is not capable of establishing a stable OCV, increasing the number of electrode lines to form an interdigitated electrode pattern increases the surface area and amount of catalyst available for the electrode reactions. An increased number of active reaction sites permits the creation of a stable difference in oxygen partial pressure between anode and cathode and thus increases the voltage stability of the cell.

3.3 Cell stacks

Cells with either one pair or five electrode pairs were assembled in a two- and three-cell stack (Fig. 1 e-f) and their performance output was compared with the corresponding single cells. The average electrode width, thickness and interelectrode distance were ~400 μm, 13 μm and 290 μm, respectively. Fig. 9a and b show the OCV as a function of time for the different stack configurations. The zero OCV of the cell with one electrode pair and an electrode width smaller than the critical size could not be compensated by adding a second cell (Fig. 9a). Nevertheless, the three-cell stack enabled the temporary establishment of an OCV. In contrast to an increased number of electrode lines and an increased electrode surface area in the case of interdigitated electrodes, stacks of cells with one line per electrode did not eliminate the problem of establishing a stable difference of oxygen partial pressure between two closely-spaced small electrodes.

When a cell with interdigitated electrodes of five lines per anode and cathode was used, an OCV with continuous fluctuations between 0.5 and 0.8 V (Fig. 9b) was established. For the two- and three-cell stack, the frequency of fluctuations diminished but the amplitude increased such that the OCV varied between 0.8 V and 0.2 V. Combining cells with five lines per electrode in a stack thus did not eliminate voltage fluctuations and instability of the single cells. Therefore no significant improvement of the voltage stability could be obtained from the stack configuration. Nonetheless, the cells with five lines per electrode delivered a sufficiently high OCV so that a power output could be measured for the single cell and the stack assembly, as summarized in Table III. Notably, the power of a two- and three-cell stack increased by factors of 2.6 and 4.3, respectively, in comparison with the single cell.

Conclusions

Single-chamber solid oxide fuel cells with coplanar electrodes are well suited for miniaturization because of their compact and flexible design. Moreover, the ohmic resistance can be significantly reduced, and the performance output enhanced, by decreasing electrode width and interelectrode gap, thus reducing the ionic transport path. However, gas intermixing between very closely-spaced microelectrodes can degrade cell performance [9, 15]. In this study, a second scale effect was uncovered in the form of a minimum electrode width below which cells with one electrode pair could not be successfully operated. For a NiO-YSZ anode and LSM-YSZ cathode with an average interelectrode gap of ~250 μm on a YSZ electrolyte substrate, the critical electrode width was identified to be ~550 μm in a methane-air mixture (R_{mix} = 2) at 700°C. Cells with electrodes smaller than that size did not yield any voltage output. For electrodes with widths near the critical size, stable operation was not possible due to fluctuations in voltage and power. Only cells with larger electrodes enabled a stable voltage and power output. However, increasing the electrode width incurs a penalty on performance due to an increase in the ohmic loss. The design criteria for SC-μSOFCs with one pair of coplanar electrodes of a certain width, w, can thus be summarized as:

$w < w_{critical}$: no OCV (2)

$w \approx w_{critical}$: OCV and power fluctuations (3)

$w > w_{critical}$: stable OCV and power output (4)

$w > w_{effective}$: increased ohmic resistance (5)

$w_{critical} < w < w_{effective}$: optimized performance (6)

In this study, the optimal electrode width was estimated to be between 550 and 847 μm.

Electrodes with widths below the critical size can nonetheless be employed in interdigitated electrode structures. By increasing the number of electrode lines per anode and cathode, the active electrode area is increased, enabling a stable cell voltage despite the small width of the single electrode lines. This result highlights a significant benefit of using interdigitated architectures over single pairs of electrodes for SC-μSOFCs. Conversely, the use of cells in stacks did not lead to any significant improvement in voltage stability.

Acknowledgements

This work has been sponsored by the Fonds Québécois de la Recherche sur la Nature et les Technologies (FQRNT) and the Canadian Foundation for Innovation. Financial support for M. Kuhn was provided by the government of Québec (Doctoral research scholarship by FQRNT).

References

[1] T. Hibino and H. Iwahara, Chem. Lett. 7 (1993) 1131-1134.
[2] T. Hibino, A. Hashimoto, T. Inoue, J. Tokuno, S. Yoshida, M. Sano, Science 288 (2000) 2031-2033.
[3] T. Suzuki, P. Jasinski, V. Petrovsky, H.U. Anderson, F. Dogan, J. Electrochem. Soc. 152 (2005) A527-A531.
[4] T. Hibino, K. Ushiki, T. Sato, Y. Kuwahara, Solid State Ionics 81 (1995) 1-3.
[5] T. Hibino, K. Ushiki, Y. Kuwahara, Solid State Ionics 91 (1996) 69-74.
[6] T. Hibino, A. Hashimoto, M. Suzuki, M. Yano, S. Yoshida, M. Sano, J. Electrochem. Soc. 149 (2002) A195-A200.
[7] X. Jacques-Bedard, T.W. Napporn, R. Roberge, M. Meunier, J. Electrochem. Soc. 154 (2007) B305-B309.
[8] B.E. Buergler, M. Ochsner, S. Vuillemin, L.J. Gauckler, J. Power Sources 171 (2007) 310-320.
[9] S.-J. Ahn, Y.-B. Kim, J. Moon, J.-H. Lee, J. Kim, J. Power Sources 171 (2007) 511-516.
[10] M. Kuhn, T. Napporn, M. Meunier, S. Vengallatore, D. Therriault, J. Micromech. Microeng. 18 (2008) 015005.
[11] M. Kuhn, T. Napporn, M. Meunier, D. Therriault, S. Vengallatore, J. Power Sources 177 (2008) 148-153.
[12] W. van Gool, Philips Res. Rep. 20 (1965) 81-93.
[13] G.A. Louis, J.M. Lee, D.L. Maricle, J.C. Trocciola, US patent 4,248,941 (1981).
[14] C.-Y. Chung and Y.-C. Chung, J. Power Sources 154 (2006) 35-41.
[15] J. Fleig, H. L. Tuller, J. Maier, Solid State Ionics 174 (2004) 261-270.
[16] Z. Shao, S.M. Haile, J. Ahn, P.D. Ronney, Z. Zhan, S.A. Barnett, Nature 435 (2005) 795-798.
[17] E.J. Crumlin, G.J. La O, Y. Shao-Horn, ECS Transactions - 10th International Symposium on Solid Oxide Fuel Cells, 7 (2007) 981-986.
[18] S.-J. Ahn, J.-H. Lee, J. Kim, J. Moon, Electrochem. Solid-State Lett. 9 (2006) A228-A231.
[19] M. Kuhn, T. Napporn, M. Meunier, D. Therriault, S. Vengallatore, Mater. Res. Soc. Symp. Proc. 972 (2007) 211-216.
[20] M. Kuhn, T. W. Napporn, M. Meunier, D. Therriault, J. Electrochem. Soc. 155 (2008) B994-B1000.
[21] T. Napporn, F. Morin, M. Meunier, Electrochem. Solid-State Lett. 7 (2004) A60-A62.
[22] T.W. Napporn, X. Jacques-Bedard, F. Morin, M. Meunier, J. Electrochem. Soc. 151 (2004) A2088-A2094.
[23] B. Morel, R. Roberge, S. Savoie, T.W. Napporn, M. Meunier, J. Power Sources 186 (2009) 89-95.
[24] X. Zhang, D.O. Hayward, D.M.P. Mingos, Catal. Lett. 86 (2003) 235-243.
[25] X. Jacques-Bedard, T.W. Napporn, R. Roberge, M. Meunier, J. Power Sources 153 (2006) 108-113.
[26] K. Asano, T. Hibino, H. Iwahara, J. Electrochem. Soc. 142 (1995) 3241-3245.

[27] I. Riess, J. Power Sources 175 (2008) 325-337.
[28] N. Nakagawa, H. Sakurai, K. Kondo, T. Morimoto, K. Hatanaka, and K. Kato, J. Electrochem. Soc. 142 (1995) 3474-3479.
[29] N. Q. Minh and T. Takahashi, *Science and technology of ceramic fuel cells*, Amsterdam: Elsevier, 1995.

Tables

Table I

Characteristics of the powders used for the direct-write microfabrication of SC-μSOFCs with coplanar electrodes.

Material	Electrode	Nominal composition	Median particle size (μm)	Density (g/cm^3)	Specific surface area (BET) (m^2/g)
NiO	Anode	High purity green NiO	0.56	6.70	6.3
YSZ	Anode	92 mol% ZrO_2, 8 mol% Y_2O_3	0.25	5.99	6.1
LSM-YSZ	Cathode	70 vol% $(La_{0.8}Sr_{0.2})_{0.98}MnO_3$, 30 vol% $(ZrO_2)_{0.92}$ $(Y_2O_3)_{0.08}$	0.56	6.19	9.7

Table II

Summary of electrode dimensions and cell performance for the fabricated SC-μSOFCs with one coplanar electrode pair.

*OCV and P_{max} for cells 9 and 10 correspond to the maximum values for voltage and power obtained within the voltage and power fluctuations.

Cell	Anode width (μm)	Cathode width (μm)	Average width (μm)	Interdistance (μm)	Average electrode area (cm^2)	Anode thickness (μm)	Cathode thickness (μm)	OCV (V)	P_{max} (mW cm^{-2})
1	107±6	80±19	93	153±11	0.00574	3.9	4.0	0	0
2	188±21	196±19	192	131±27	0.01199	7.7	8.5	0	0
3	174±14	211±24	192	144±21	0.01144	3.5	4.7	0	0
4	192±11	210±26	201	145±28	0.01268	8.1	7.0	0	0
5	180±23	250±50	215	257±34	0.01364	5.8	5.6	0	0
6	461±59	420±34	441	215±60	0.02753	6.7	10.7	0	0
7	450±18	468±37	459	186±58	0.02859	7.6	13.6	0	0
8	591±39	483±37	537	322±68	0.03374	12.8	13.9	0	0
9*	574±124	535±100	554	252±85	0.03338	23.0	22.8	0.898*	10.462*
10*	581±72	533±114	557	241±86	0.03272	18.5	23.3	0.878*	9.965*
11	745±126	949±161	847	305±129	0.05239	31.8	35.9	0.860	5.106
12	785±142	931±88	858	431±120	0.05219	34.3	48.3	0.865	4.886
13	772±157	968±187	870	400±166	0.05364	29.7	38.5	0.816	3.599

14	1248±147	1357±152	1303	267±148	0.08174	38.1	49.2	0.819	2.059
15	1200±151	1561±342	1380	274±145	0.08644	38.8	51.2	0.808	1.236

Table III

Performance of cell stacks with 5 lines per electrode.

Cell	OCV (V)	P_{max} (mW)
Single cell	0.833	0.178
2-cell stack	0.789	0.461
3-cell stack	0.801	0.760

Figure Captions:

Figure 1: Optical micrographs of SC-μSOFCs with single electrode pair (average electrode width of a) 201 μm and b) 537 μm) and with c) two and d) five pairs of electrodes. Stack of three cells with e) one line per electrode and f) five lines per electrode.

Figure 2: a) Schematic representation of the cell holder, where the SC-μSOFC with coplanar electrodes is placed between a support plate and a gas distribution plate. b) Photograph of the lower side of the gas distribution plate facing the cell. Holes are machined into the plate to let the reaction gases access the cell underneath, whereas the posts are to enhance mixing of the reactant gases flowing over the electrodes.

Figure 3: Representative time-dependent behavior of the OCV for cells with one electrode pair of different average electrode widths (93, 557 and 1380 μm) at 700°C, R_{mix} = 2 and a total gas flow of 150 sccm.

Figure 4: a) Open circuit voltage and b) maximum power density as a function of average electrode width for cells with a single electrode pair. The tests were performed at 700°C, R_{mix} = 2 and a total gas flow of 150 sccm. ▲Δ and ▼ correspond to the maximum and minimum value of the OCV and maximum power density obtained for the unstable cells with fluctuating voltage.

Figure 5: a) Cell voltage and b) power density against current density for cells with a single electrode pair delivering a non-zero OCV at 700°C, R_{mix} = 2 and a total gas flow of 150 sccm.

Figure 6: a) Optical micrograph of anode and cathode after testing (average electrode width: 858 μm). The anode exhibited a white color in the region closest to the cathode and at the tip. b) Representative SEM micrograph of tested anode in region away from interelectrode gap and c) in white region close to the gap.

Figure 7: Schematic representation of design criteria for SC-μSOFCs with one coplanar electrode pair.

Figure 8: Representative time-dependent behavior of the OCV for cells with a) one, two, three and b) four, five and ten pairs of interdigitated electrodes. The OCV was measured at 700°C, R_{mix} = 2 and a total gas flow of 150 sccm.

Figure 9: Representative time-dependent behavior of the OCV for cells with a) one and b) five electrode pairs as a single cell and assembled in a two-cell and three-cell stack. The OCV was measured at 700°C, R_{mix} = 2 and a total gas flow of 150 sccm.

Figure 1:

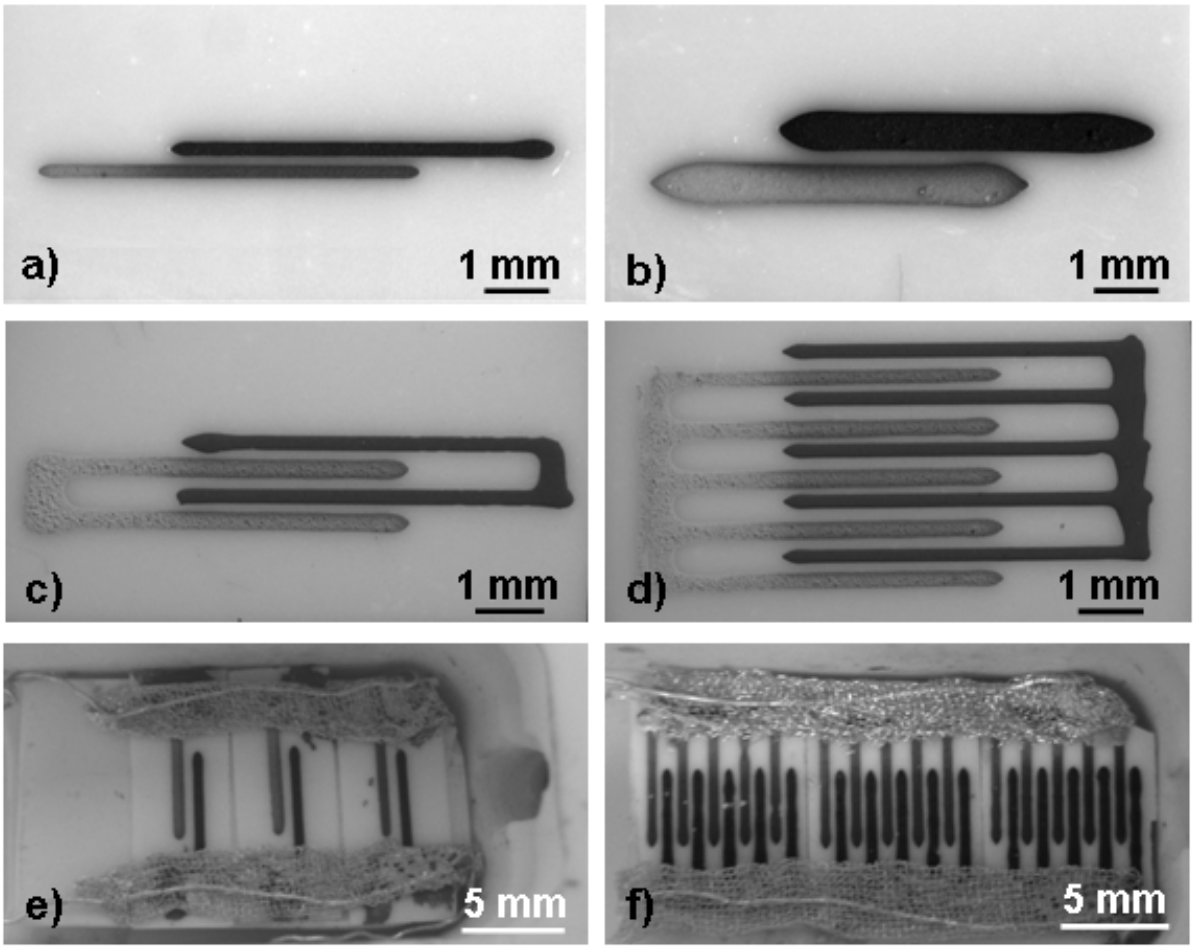

Figure 2:

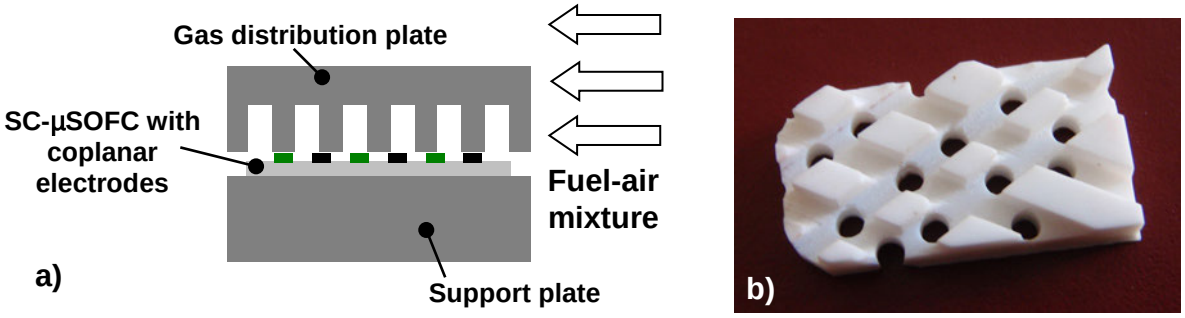
Gas distribution plate
SC-µSOFC with coplanar electrodes
Fuel-air mixture
a)
Support plate
b)

Figure 3:

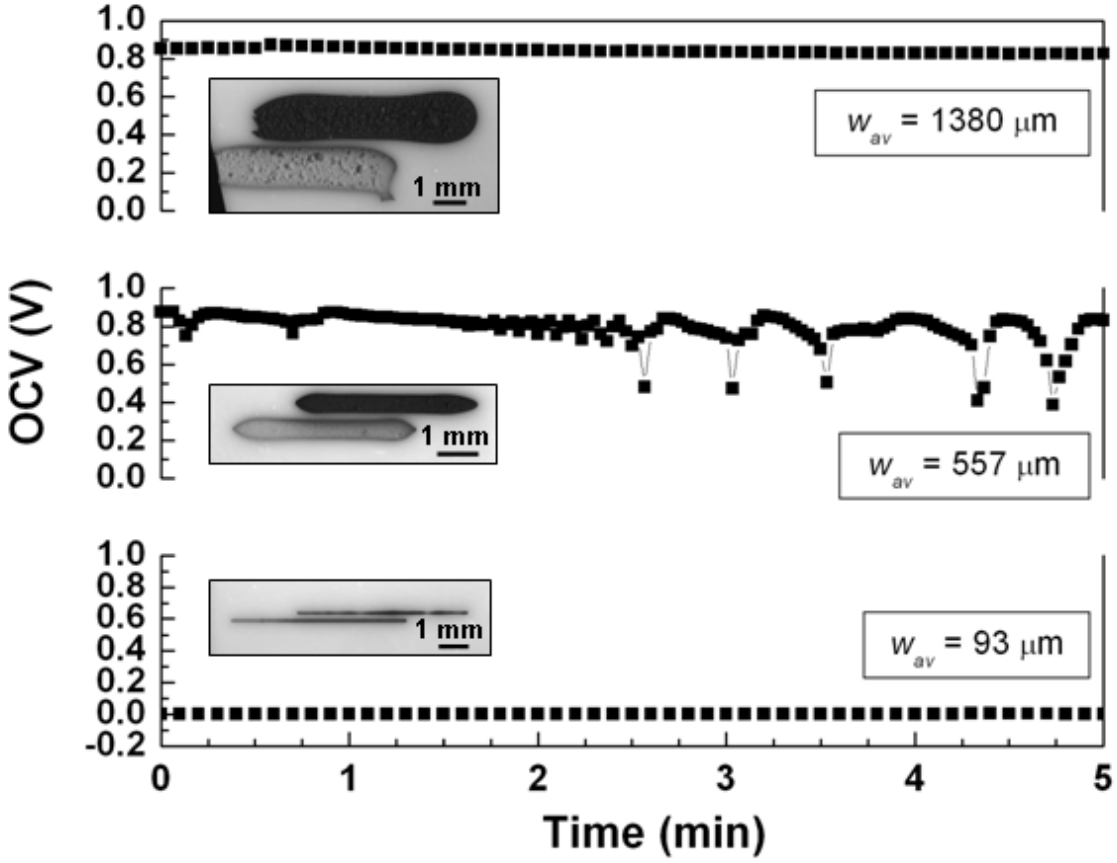

Figure 4a:

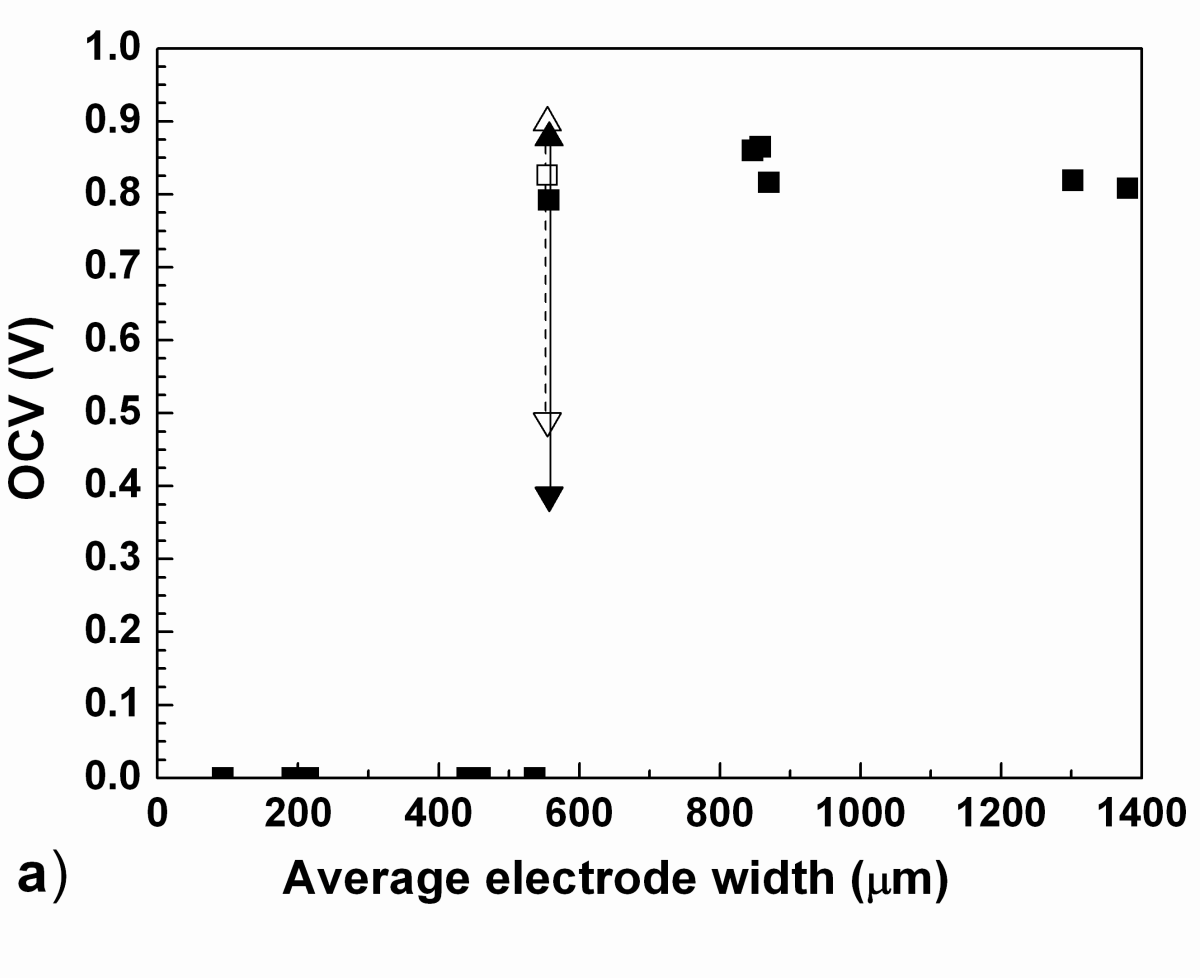
1.0
0.9
0.8
0.7
0.6
0.5
0.4
0.3
0.2
0.1
0.0
OCV (V)
0
200
400
600
800
1000
1200
1400
a)
Average electrode width (μm)

Figure 4b:

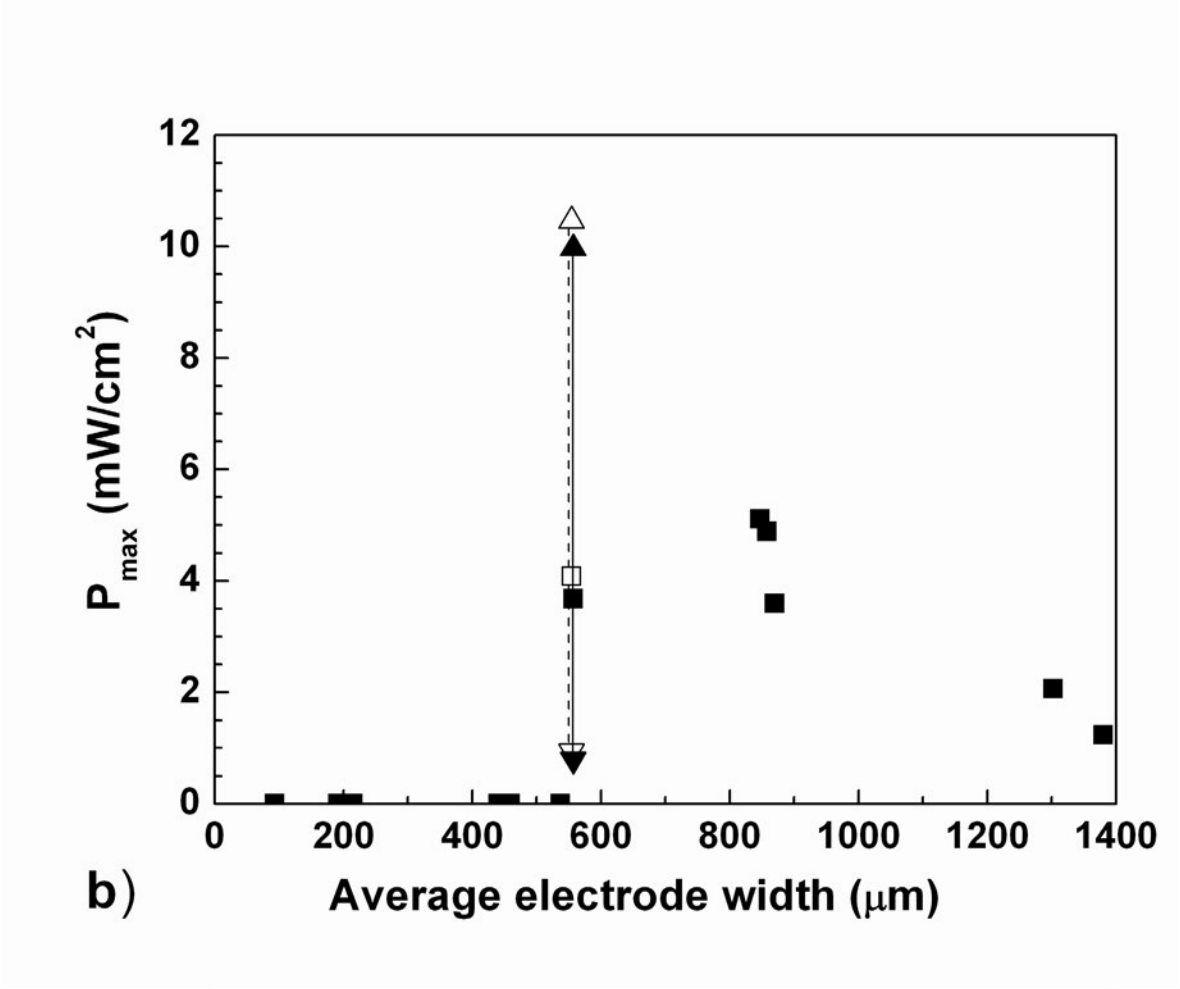
12
10
8
6
4
2
0
P_{max} (mW/cm^2)
0
200
400
600
800
1000
1200
1400
b)
Average electrode width (μm)

Figure 5a:

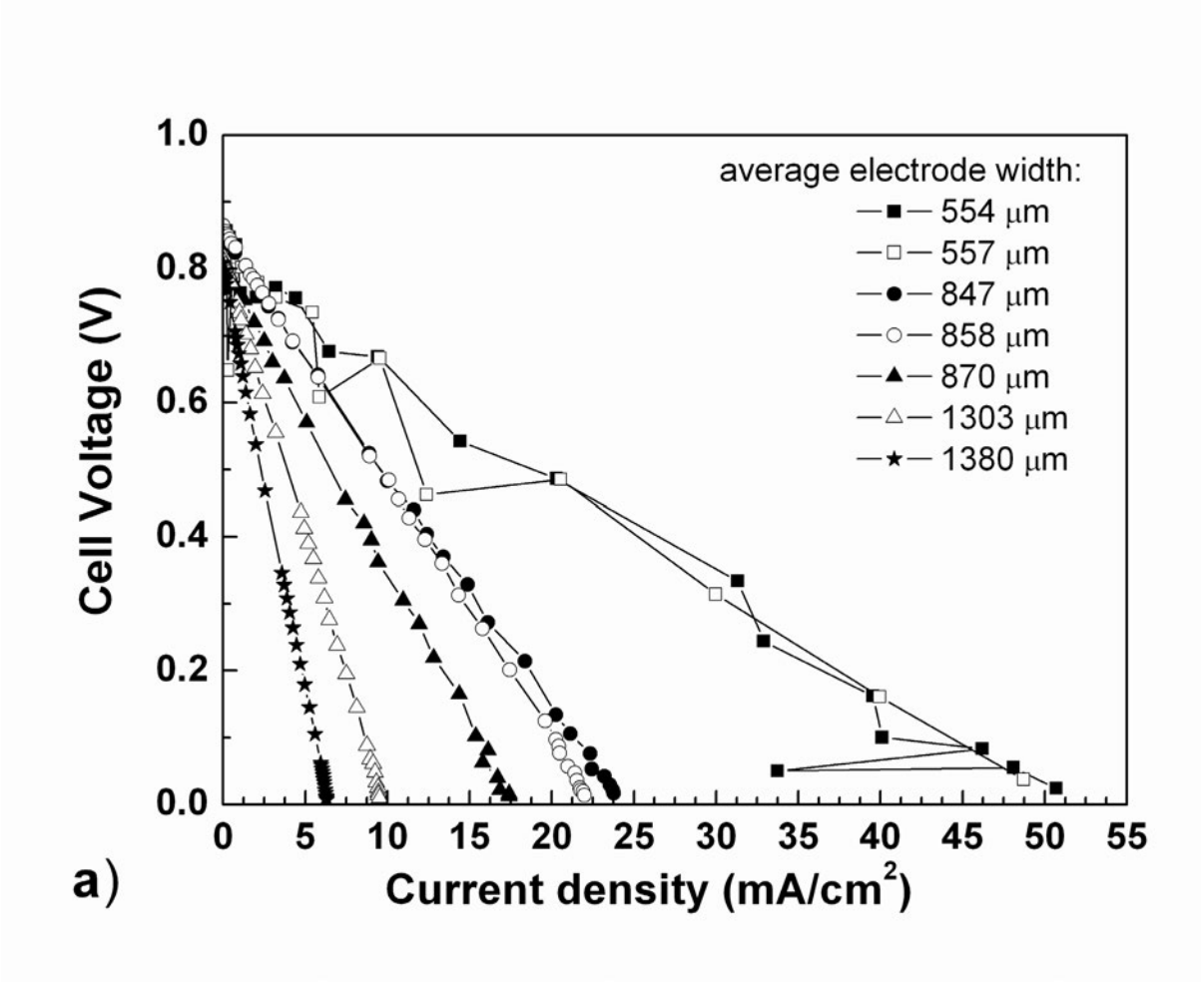
1.0
0.8
0.6
0.4
0.2
0.0
Cell Voltage (V)
0
5
10
15
20
25
30
35
40
45
50
55
Current density (mA/cm^2)
a)
average electrode width:
554 μm
557 μm
847 μm
858 μm
870 μm
1303 μm
1380 μm

Figure 5b:

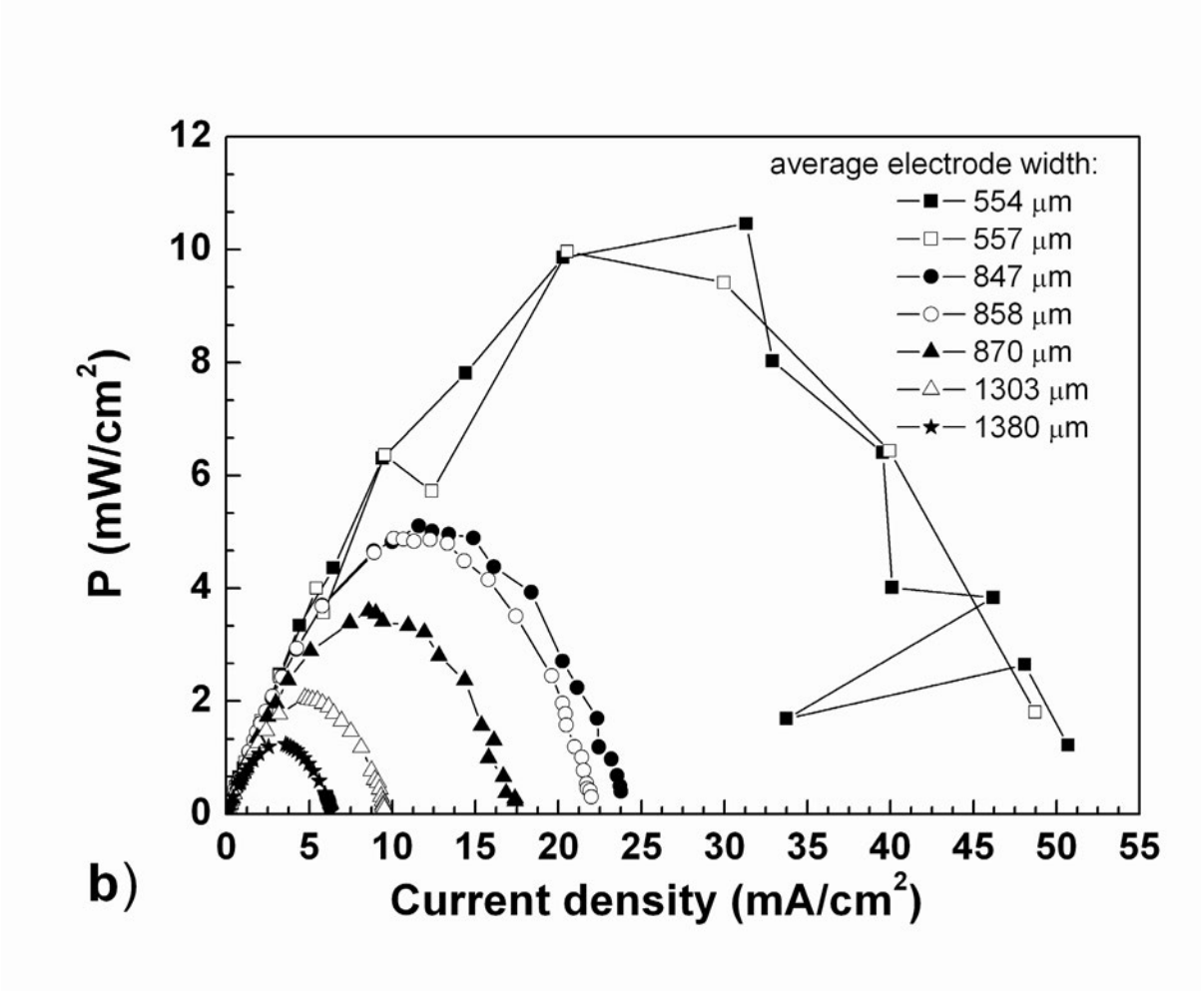
b)
P (mW/cm^2)
Current density (mA/cm^2)
average electrode width:
554 μm
557 μm
847 μm
858 μm
870 μm
1303 μm
1380 μm
0
2
4
6
8
10
12
0
5
10
15
20
25
30
35
40
45
50
55

Figure 6:

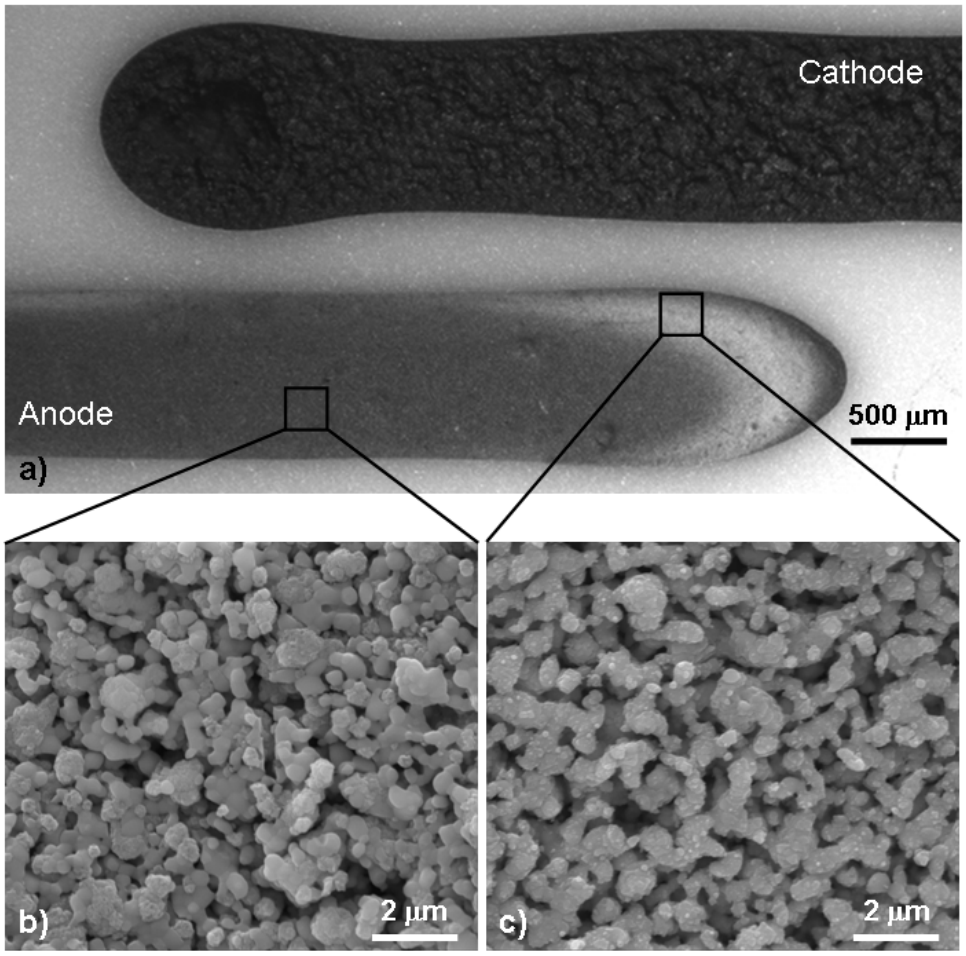

Figure 7:

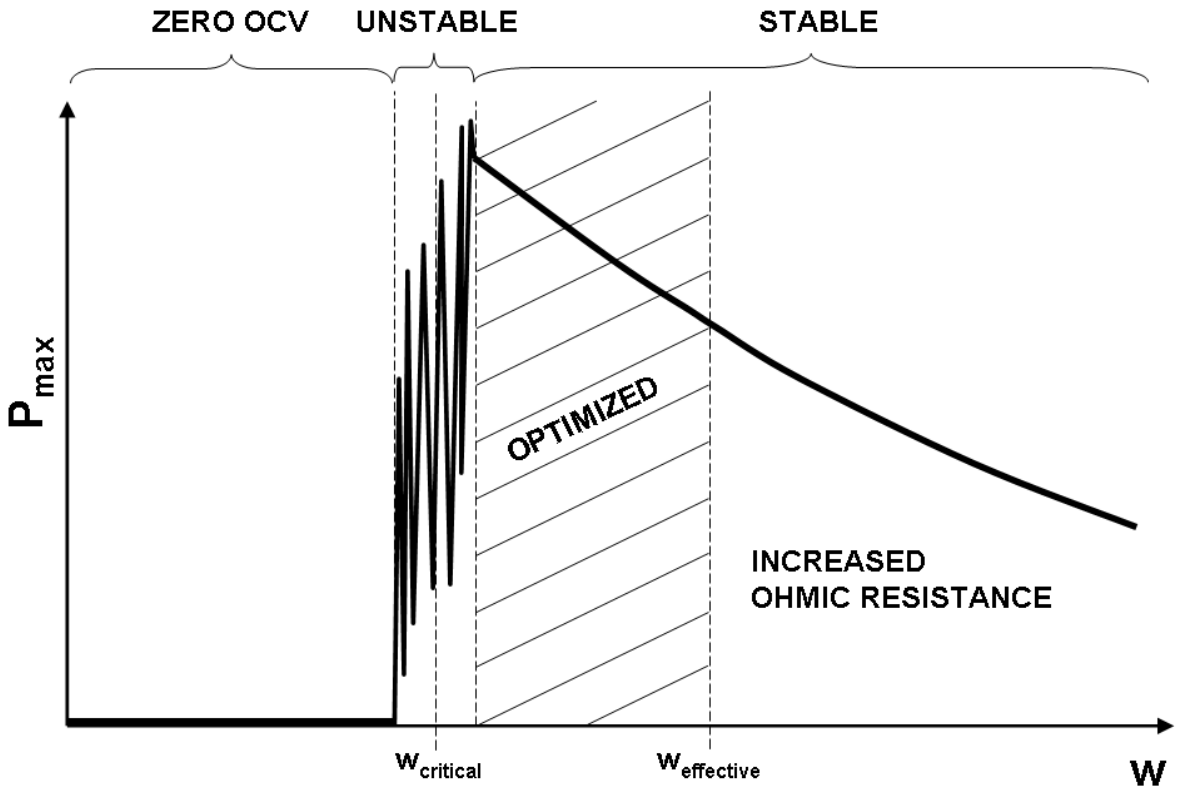
ZERO OCV
UNSTABLE
STABLE
P max
OPTIMIZED
INCREASED
OHMIC RESISTANCE
W critical
W effective
W

Figure 8a:

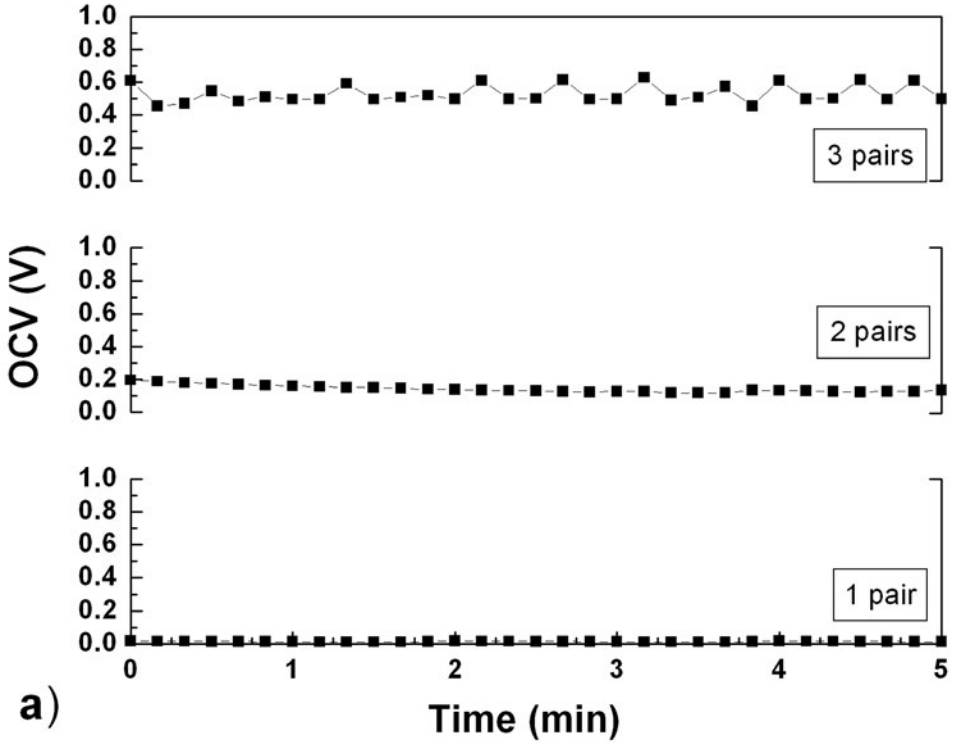

Figure 8b:

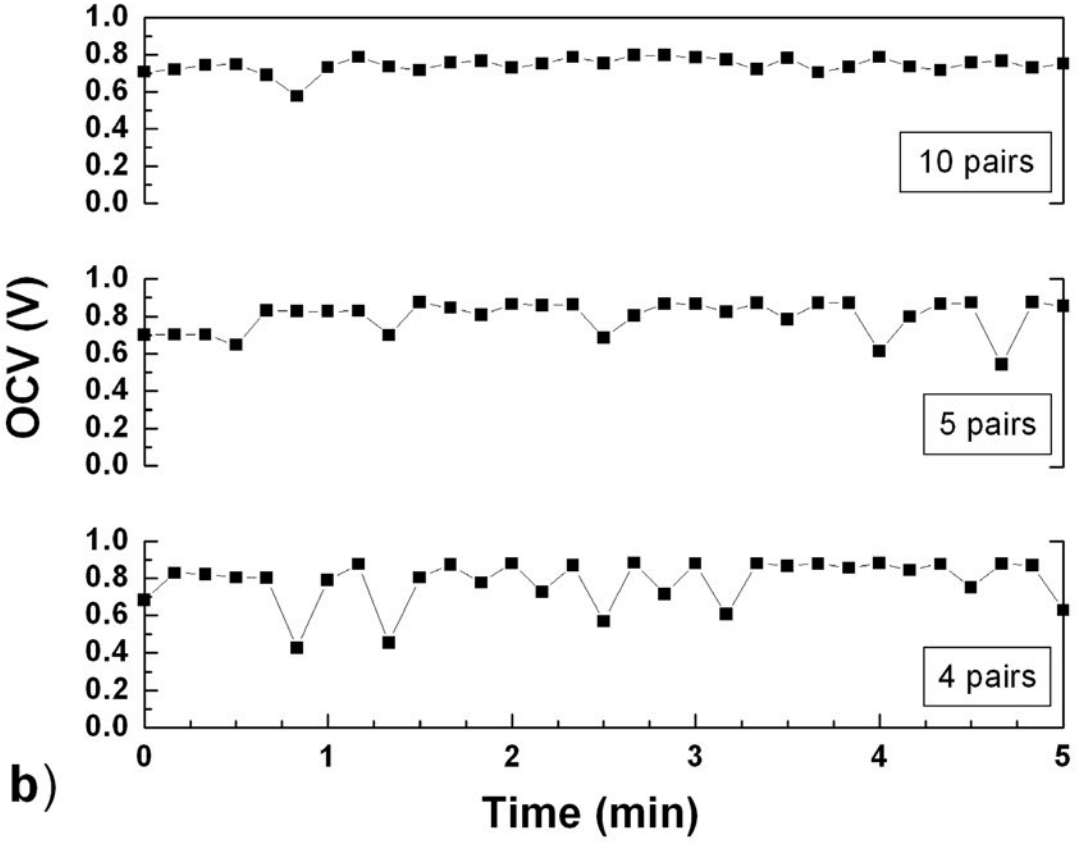

Figure 9a:

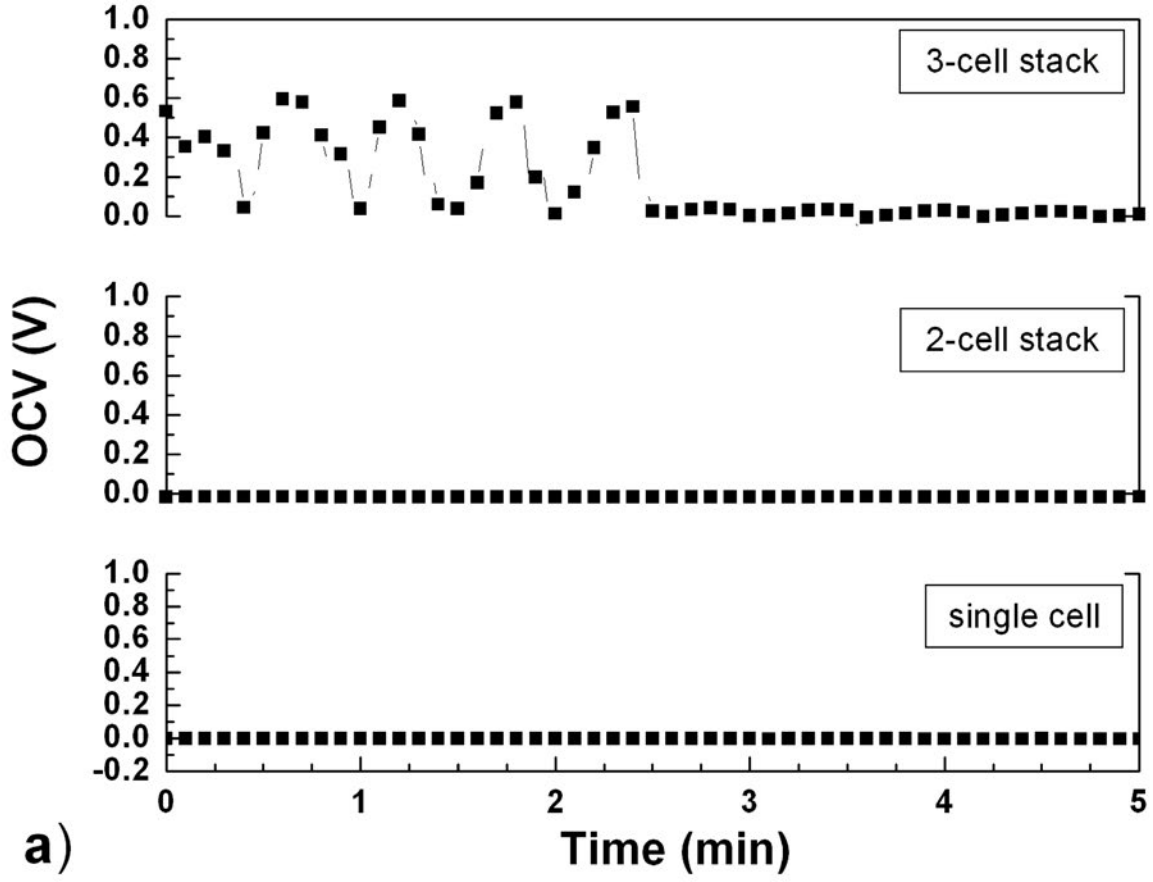

Figure 9b:

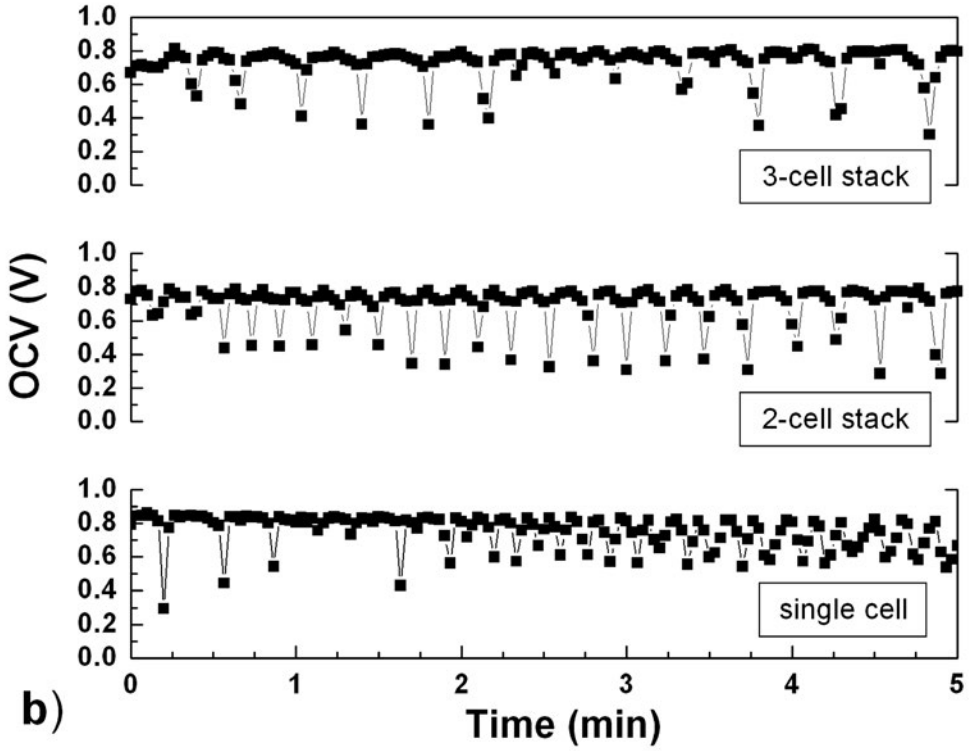
1.0
0.8
0.6
0.4
0.2
0.0
3-cell stack
2-cell stack
single cell
OCV (V)
0
1
2
3
4
5
Time (min)
b)